Supplementary Figure Legends

Supplementary Figure 1. Serum miR-23a level was highly correlated with tissue Ki-67 expression in melanoma patients. (A, B) qRT-PCR measurements of serum miR-23a level of melanoma patients and cancer-free controls. Data represent the mean ± SD in simple bar chart. **(C)** Immunohistochemistry analysis of Ki-67 staining score in 100 primary melanoma tissues and 92 metastatic melanoma tissues. *P* value was calculated by two-tailed Student's t-test. **P* < 0.05. **(D)** Representative immunohistochemistry images of Ki-67 in primary melanoma and metastatic melanoma. Scale bar = 100μm. **(E)** Correlation between serum miR-23 level and Ki-67 staining score was tested by Spearman's rank correlation analysis, with r and *P* values indicated. *P* value was calculated by two-tailed Student's *t*-test. **P* < 0.05, ****P* < 0.001.

Supplementary Figure 2. Overexpression of miR-23a has minimal impact on melanoma cell proliferation and cell apoptosis. (A, B) The level of miR-23a was tested by qRT-PCR in the indicated cell lines following transfection with miR-23a or control miRNA. Data represent the mean ± SD of triplicates. **(C, D)** Growth curves of A2058 cells and A375 cells with or without miR-23a overexpression. Data represent the mean ± SD of triplicates. **(E, F)** Flow cytometry analysis of apoptotic A2058 and A375 cells with or without miR-23a overexpression. Data represent the mean ± SD of triplicates. NS, non-significant. **(G)** P53 protein expressions

measured in A2058 and A375 cells with or without miR-23a overexpression. Actin was used for normalization. Data represent the mean ± SD of triplicates. NS, non-significant. *P* value was calculated by two-tailed Student's *t*-test. $^{**}P < 0.01$.

Supplementary Figure 3. Suppression of autophagy inhibits melanoma invasion and migration. (A) The protein expression of ATG5, LC3 and p62 was evaluated by western blot in A2058 cells transfected with *ATG5* siRNA or control siRNA. Actin was detected as loading control. Data represent the mean ± SD of triplicates. **(B)** The protein expression of LC3 and p62 was evaluated by western blot in A2058 cells treated with 5μM 3-MA or control. Actin was detected as loading control. Data represent the mean ± SD of triplicates. **(C, D)** A2058 cells treated with 5μM 3-MA or control were subjected to matrigel invasion and transwell migration assay. Representative fields of the invaded and migrated cells are shown. Scale bar = 100μm. The invaded and migrated cells were also quantified on the right. Data represent the mean ± SD of triplicates. **(E)** A2058 cells treated with 5μM 3-MA or control were subjected to the wound-healing assay. Experiments were repeated three times with similar results. Scale bar = 100μm. **(F)** Quantification of protein expressions related to Fig. 3E. Data represent the mean ± SD of triplicates. **(G)** Venn diagram depicting the number of miR-23a targets predicted by bioinformatics tools, including miRanda, miRWalk, Targetscan and DIANAmicroT. *P* value was calculated by two-tailed Student's *t*-test. $^{**}P < 0.01$, $^{***}P < 0.001$.

Supplementary Figure 4. ATG12 expression in primary melanoma and metastatic melanoma. (A) Representative immunohistochemistry images of ATG12 in primary melanoma and metastatic melanoma. Scale bar = 100μm. **(B)** Immunohistochemistry analysis of ATG12 staining score in 43 primary melanoma tissues and 23 metastatic melanoma tissues. *P* value was calculated by two-tailed Student's *t*-test. **P* < 0.05. **(C)** Correlation between serum miR-23 level and Ki-67 staining score was tested by Spearman's rank correlation analysis, with r and *P* values indicated.

Supplementary Figure 5. MiR-23a regulates the invasive and migratory ability of melanoma cells through autophagy. (**A, B**) A2058 cells treated as indicated were subjected to the matrigel invasion and transwell migration assay. Representative fields of the invaded and migrated cells are shown. Scale bar = 100μm. The invaded and migrated cells were also quantified on the right. Data represent the mean ± SD of triplicates. *P* value was calculated by two-tailed Student's *t*-test. **P* < 0.05.

Supplementary Figure 6. mRNA levels of EMT-related genes in A2058 cells transfected with indicated vectors. Data represent the mean ± SD of triplicates. *P* value was calculated by two-tailed Student's *t*-test. NS, non-significant.

Supplementary Figure 7. MiR-23a-ATG12 axis regulated AMPK signaling. (A)

Assessment of ATP level in ATG12-silenced and miR-23a-overexpressed A375 cells. Data represent the mean ± SD of triplicates. **(B)** Immunoblotting analysis of AMPKα, phosphorylated-AMPKα and phosphorylated-ACC protein expression in A375 cells treated as indicated. Actin was used for normalization. NC, negative control. **(C)** Quantification of protein expressions related to Fig. 5B. Data represent the mean ± SD of triplicates. **(D)** Quantification of protein expressions related to Supplementary Fig. 7B. Data represent the mean ± SD of triplicates. **(E)** Immunoprecipitation analysis of the interaction between ATG12 and AMPK. **(F)** The cell viability of A2058 and A375 cells treated with indicated concentrations of Compound C (CC). Data represent the mean ± SD of triplicates. NS, non-significant. **(G)** Immunoblotting analysis of AMPKα, phosphorylated-AMPKα and phosphorylated-ACC protein expression in A2058 and A375 cells treated with indicated concentrations of Compound C. Actin was used for normalization. *P* value was calculated by two-tailed Student's *t*-test. $^{**}P < 0.01$, $^{***}P < 0.001$.

Supplementary Figure 8. MiR-23a-ATG12 axis suppresses melanoma invasion and metastasis through autophagy-mediated AMPK signaling. (A, B) si*ATG12*-A375 cells treated with control or Compound C were subjected to the cell invasion and migration assay. Representative fields of the invaded and migrated cells are shown. Scale bar = 100μm. The invaded and migrated cells were quantified on the right. Data represent the mean ± SD of triplicates. NC, negative control. CC, Compound C. **(C)** si*ATG12*-A375 cells treated with or without Compound C were

subjected to wound-healing assay. Experiments were repeated three times with similar results. Scale bar = 100μm. **(D, E)** miR-23a-overexpressed A375 cells treated with or without Compound C were subjected to the cell invasion and migration assay. Representative fields of the invaded and migrated cells are shown. Scale bar = 100μm. The invaded and migrated cells were quantified on the right. Data represent the mean ± SD of triplicates. **(F)** miR-23a-overexpressed A375 cells treated with or without Compound C were subjected to wound-healing assay. Experiments were repeated three times with similar results. Scale bar = 100μm. *P* value was calculated by two-tailed Student's *t*-test. **P* < 0.05, ***P* < 0.01.

Supplementary Figure 9. RhoA mediated melanoma invasion and migration downstream of AMPK. (A) The expression of RhoA and phosphorylated-RhoA was detected by western blotting in A2058 and A375 cells treated with or without Compound C. Actin was used as the internal standard. Data represent the mean ± SD of triplicates. NC, negative control. CC, Compound C. **(B)** Immunoblotting analysis of RhoA expression in A2058 cells transfected with siRNAs against *RhoA*. Actin was used for normalization. **(C, D)** A2058 cells treated as indicated were subjected to the cell invasion and migration assay. Representative fields of the invaded and migrated cells are shown. Scale bar = 100μm. The invaded and migrated cells were quantified on the right. Data represent the mean ± SD of triplicates. **(E, F)** A375 cells treated as indicated were subjected to the cell invasion and migration assay. Representative fields of the invaded and migrated cells are

shown. Scale bar = 100μm. The invaded and migrated cells were quantified on the right. Data represent the mean ± SD of triplicates. *P* value was calculated by two-tailed Student's *t*-test. *$P < 0.05$, **$P < 0.01$.

Supplementary Figures

Supplementary Figure 1

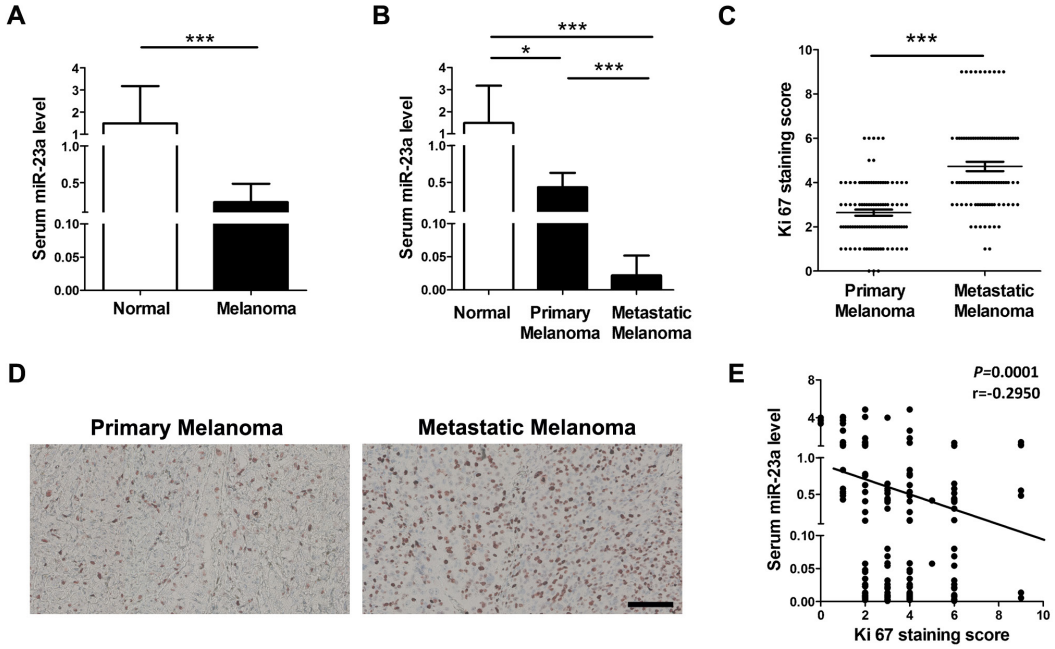

Supplementary Figure 2

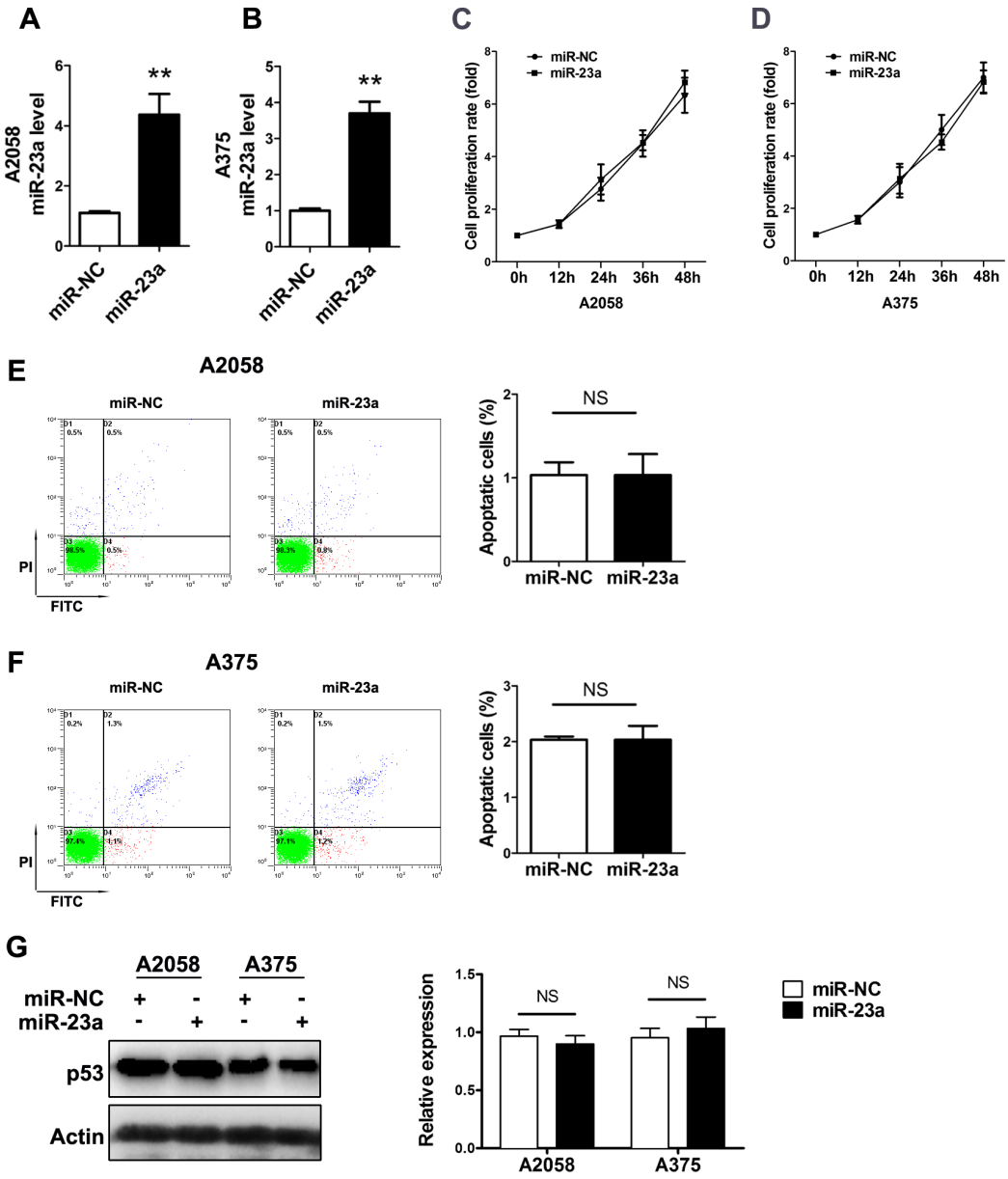

Supplementary Figure 3

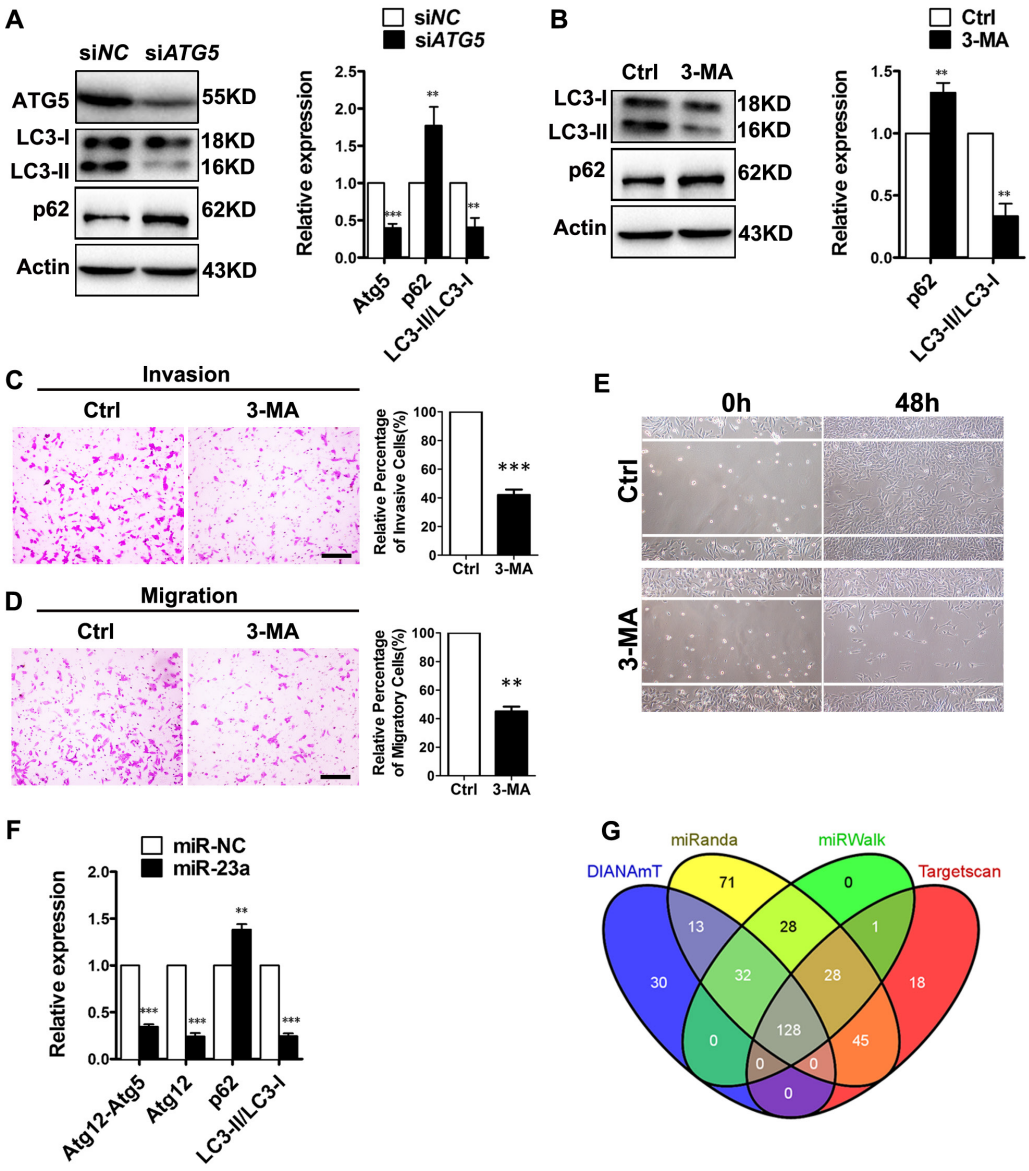

Supplementary Figure 4

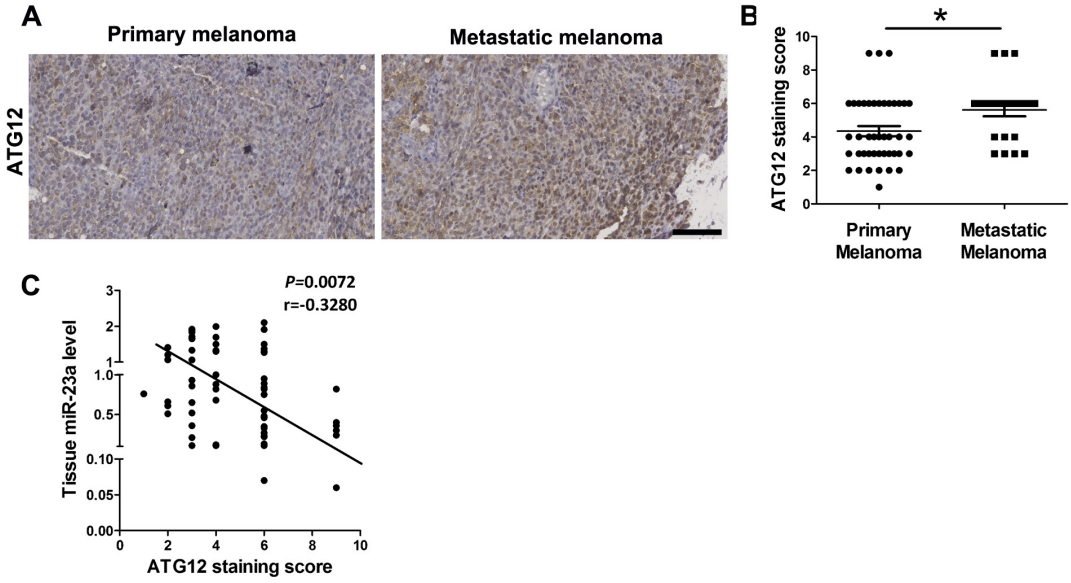

Supplementary Figure 5

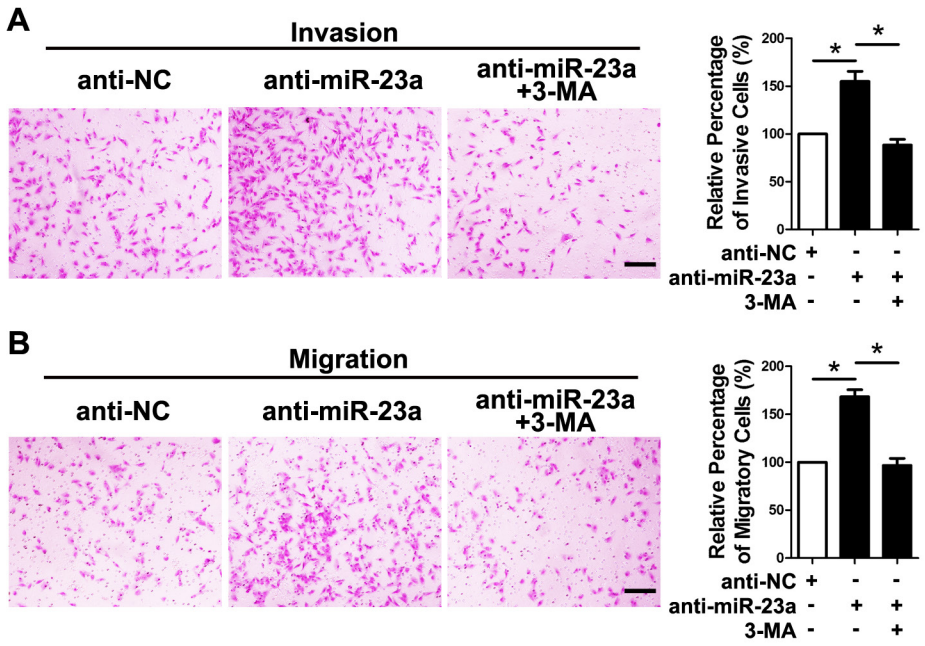

Supplementary Figure 6

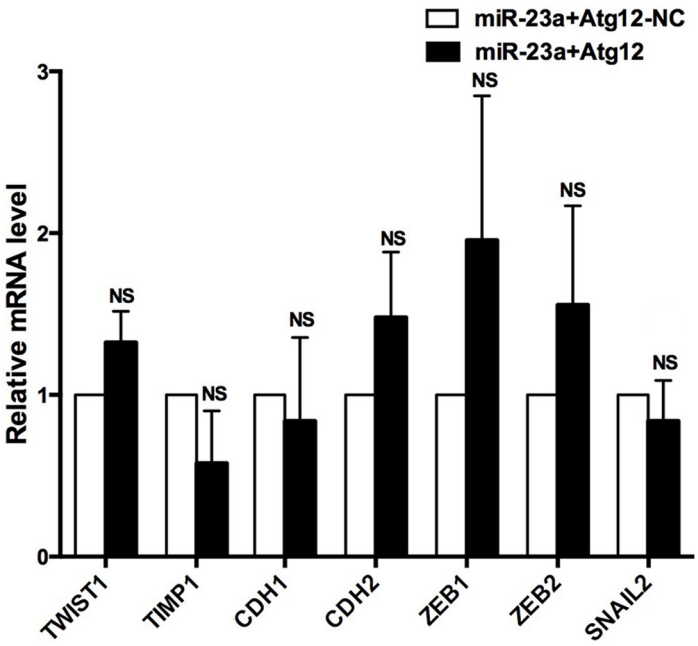

Supplementary Figure 7

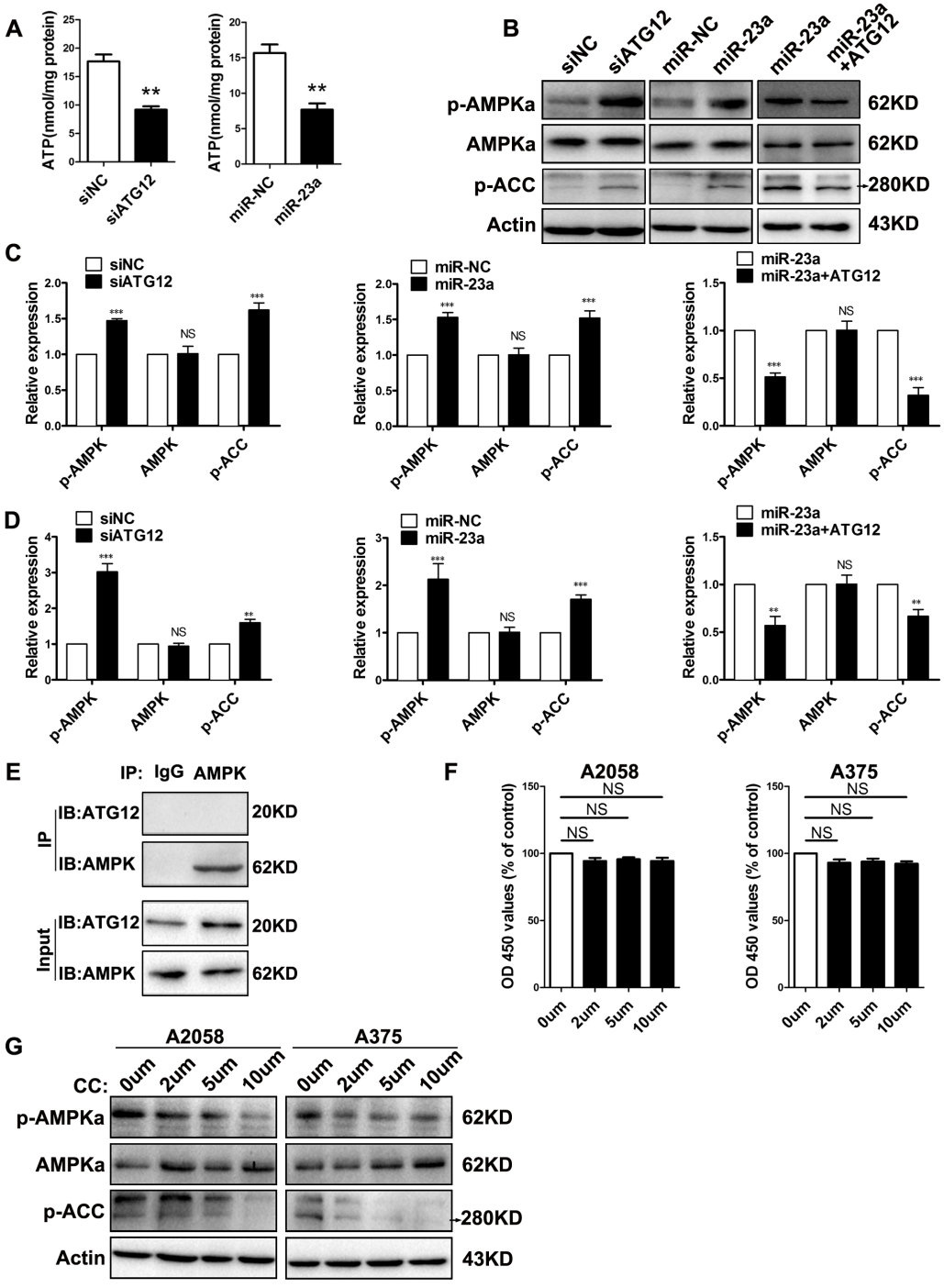

Supplementary Figure 8

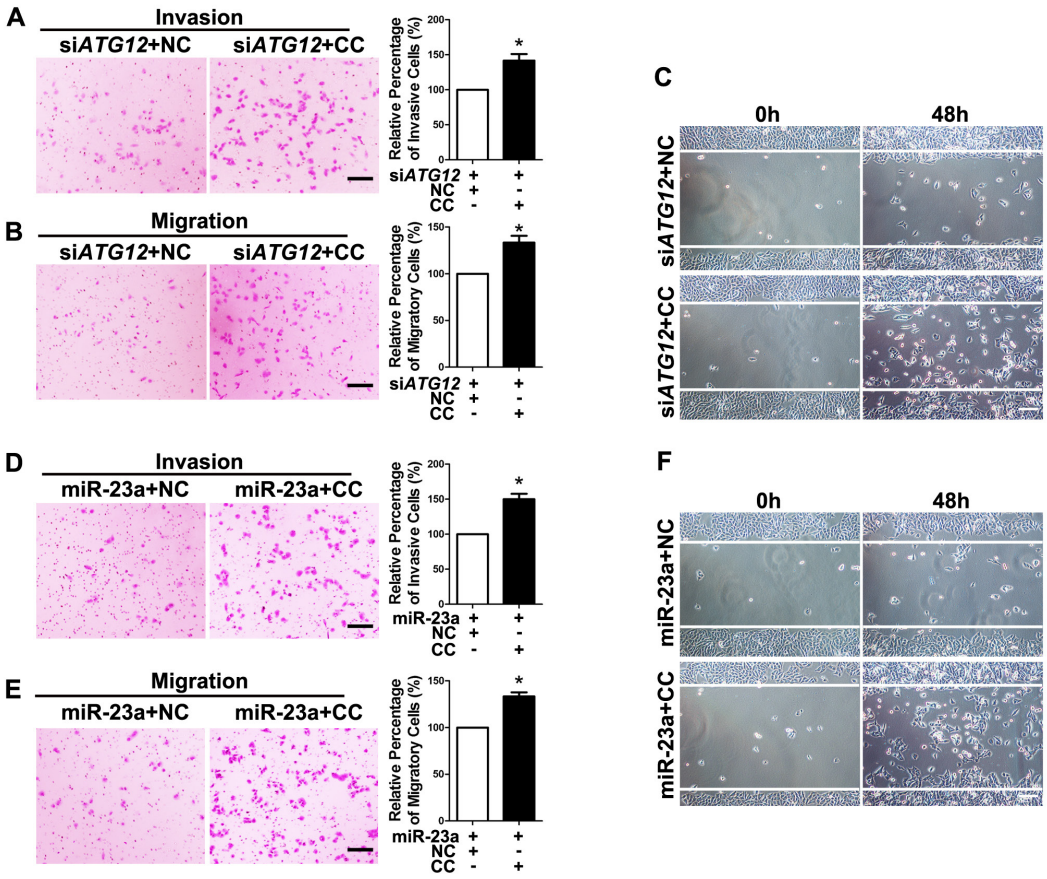

Supplementary Figure 9

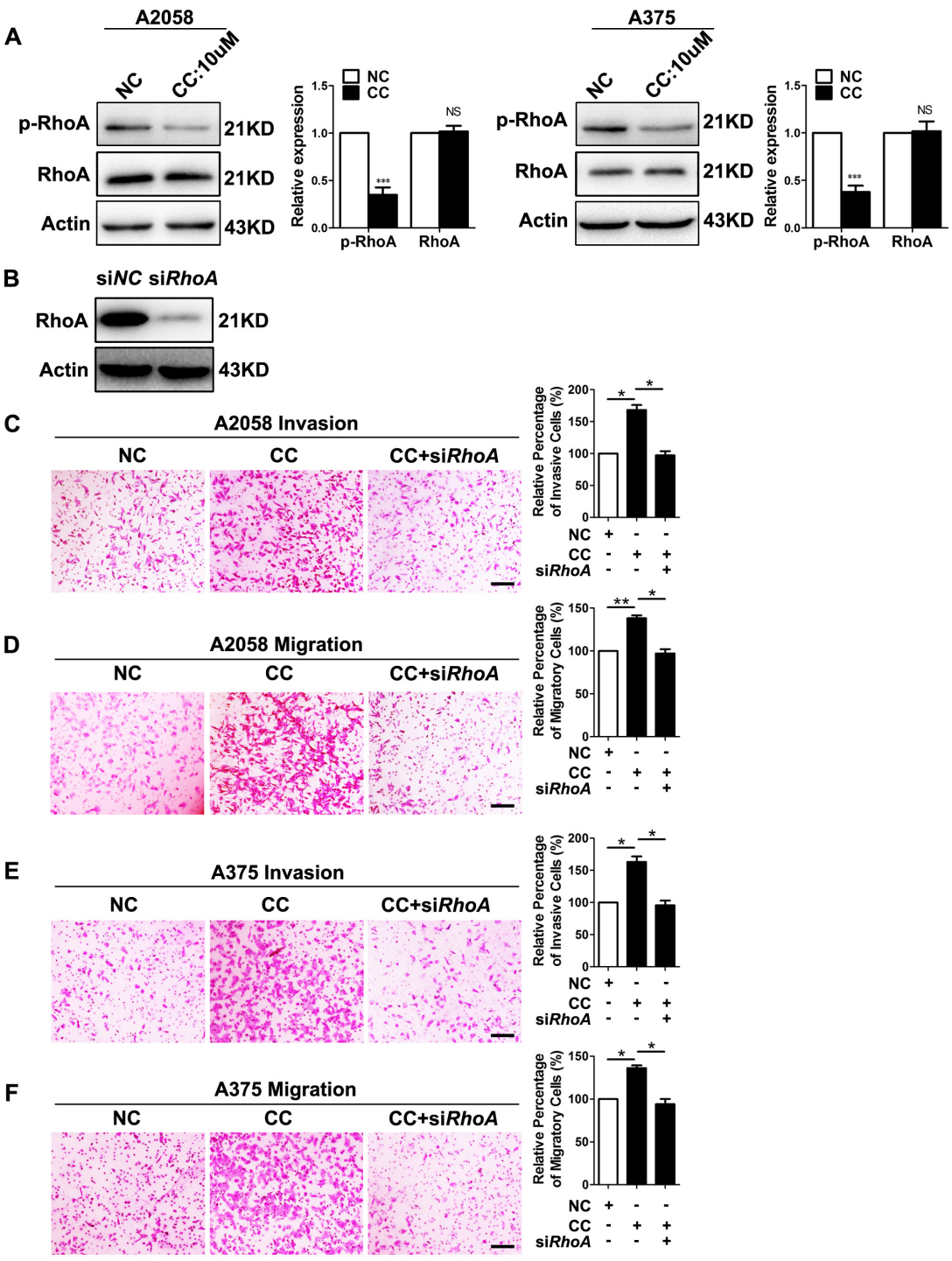

Supplementary Tables

Supplementary Table 1. Detailed Information of target-gene scan of miR-23a

	MicroRNA	Target Gene	DIANAmT	miRanda	miRWalk	Targetscan
1	hsa-miR-23a	RFXDC1	1[#]	1	1	1
2	hsa-miR-23a	SEC23A	1	1	1	1
3	hsa-miR-23a	BLCAP	1	1	1	1
4	hsa-miR-23a	BTBD14A	1	1	1	1
5	hsa-miR-23a	ATG12	1	1	1	1
6	hsa-miR-23a	NCOA6	1	1	1	1
7	hsa-miR-23a	FUT4	1	1	1	1
8	hsa-miR-23a	TIPARP	1	1	1	1
9	hsa-miR-23a	INTU	1	1	1	1
10	hsa-miR-23a	HOXD10	1	1	1	1
11	hsa-miR-23a	SPOPL	1	1	1	1
12	hsa-miR-23a	CRBN	1	1	1	1
13	hsa-miR-23a	GPRC5B	1	1	1	1
14	hsa-miR-23a	POU4F2	1	1	1	1
15	hsa-miR-23a	LGR4	1	1	1	1
16	hsa-miR-23a	AMBRA1	1	1	1	1
17	hsa-miR-23a	ZBTB26	1	1	1	1
18	hsa-miR-23a	TBC1D15	1	1	1	1
19	hsa-miR-23a	UTX	1	1	1	1

20	hsa-miR-23a	SEMA6D	1	1	1	1
21	hsa-miR-23a	CAPN6	1	1	1	1
22	hsa-miR-23a	EIF3A	1	1	1	1
23	hsa-miR-23a	CCNH	1	1	1	1
24	hsa-miR-23a	GNPDA1	1	1	1	1
25	hsa-miR-23a	PPIF	1	1	1	1
26	hsa-miR-23a	TRIB1	1	1	1	1
27	hsa-miR-23a	SPRY2	1	1	1	1
28	hsa-miR-23a	MAB21L2	1	1	1	1
29	hsa-miR-23a	CTCF	1	1	1	1
30	hsa-miR-23a	PPARGC1A	1	1	1	1
31	hsa-miR-23a	CPSF4	1	1	1	1
32	hsa-miR-23a	PNRC1	1	1	1	1
33	hsa-miR-23a	B3GNT1	1	1	1	1
34	hsa-miR-23a	PROSC	1	1	1	1
35	hsa-miR-23a	SLC6A14	1	1	1	1
36	hsa-miR-23a	KLF12	1	1	1	1
37	hsa-miR-23a	CHUK	1	1	1	1
38	hsa-miR-23a	OSBPL8	1	1	1	1
39	hsa-miR-23a	TADA1L	1	1	1	1
40	hsa-miR-23a	C12orf54	1	1	1	1
41	hsa-miR-23a	ADH5	1	1	1	1

42	hsa-miR-23a	COL4A5	1	1	1	1
43	hsa-miR-23a	ASB15	1	1	1	1
44	hsa-miR-23a	TTC7B	1	1	1	1
45	hsa-miR-23a	CSNK2A2	1	1	1	1
46	hsa-miR-23a	ANKRD29	1	1	1	1
47	hsa-miR-23a	CCDC52	1	1	1	1
48	hsa-miR-23a	FAM134C	1	1	1	1
49	hsa-miR-23a	DHX15	1	1	1	1
50	hsa-miR-23a	DLX1	1	1	1	1
51	hsa-miR-23a	ELF2	1	1	1	1
52	hsa-miR-23a	FLJ38973	1	1	1	1
53	hsa-miR-23a	EPS15	1	1	1	1
54	hsa-miR-23a	KCTD20	1	1	1	1
55	hsa-miR-23a	RAB11FIP2	1	1	1	1
56	hsa-miR-23a	ZBTB1	1	1	1	1
57	hsa-miR-23a	CD93	1	1	1	1
58	hsa-miR-23a	MAPRE1	1	1	1	1
59	hsa-miR-23a	PDXDC1	1	1	1	1
60	hsa-miR-23a	ZNF423	1	1	1	1
61	hsa-miR-23a	CAMTA1	1	1	1	1
62	hsa-miR-23a	BICD2	1	1	1	1
63	hsa-miR-23a	SATB2	1	1	1	1

64	hsa-miR-23a	ZDHHC17	1	1	1	1
65	hsa-miR-23a	ZNF281	1	1	1	1
66	hsa-miR-23a	TTC33	1	1	1	1
67	hsa-miR-23a	WBP2	1	1	1	1
68	hsa-miR-23a	STX12	1	1	1	1
69	hsa-miR-23a	FRK	1	1	1	1
70	hsa-miR-23a	VGLL2	1	1	1	1
71	hsa-miR-23a	MAP3K7IP3	1	1	1	1
72	hsa-miR-23a	ASF1A	1	1	1	1
73	hsa-miR-23a	ODZ4	1	1	1	1
74	hsa-miR-23a	GLCE	1	1	1	1
75	hsa-miR-23a	INTS6	1	1	1	1
76	hsa-miR-23a	NAP1L5	1	1	1	1
77	hsa-miR-23a	GJA1	1	1	1	1
78	hsa-miR-23a	FILIP1	1	1	1	1
79	hsa-miR-23a	ARFIP1	1	1	1	1
80	hsa-miR-23a	BBS9	1	1	1	1
81	hsa-miR-23a	TNRC6A	1	1	1	1
82	hsa-miR-23a	GNAI1	1	1	1	1
83	hsa-miR-23a	GPR22	1	1	1	1
84	hsa-miR-23a	EFHA2	1	1	1	1
85	hsa-miR-23a	DPY19L4	1	1	1	1

86	hsa-miR-23a	C16orf72	1	1	1	1
87	hsa-miR-23a	MDFIC	1	1	1	1
88	hsa-miR-23a	HOXB4	1	1	1	1
89	hsa-miR-23a	IDH1	1	1	1	1
90	hsa-miR-23a	PLCXD3	1	1	1	1
91	hsa-miR-23a	FAS	1	1	1	1
92	hsa-miR-23a	IL6R	1	1	1	1
93	hsa-miR-23a	IL11	1	1	1	1
94	hsa-miR-23a	IRF2	1	1	1	1
95	hsa-miR-23a	ITGB8	1	1	1	1
96	hsa-miR-23a	JARID2	1	1	1	1
97	hsa-miR-23a	KCNK3	1	1	1	1
98	hsa-miR-23a	KPNA1	1	1	1	1
99	hsa-miR-23a	KPNA4	1	1	1	1
100	hsa-miR-23a	LAMP1	1	1	1	1
101	hsa-miR-23a	LBR	1	1	1	1
102	hsa-miR-23a	LRP5	1	1	1	1
103	hsa-miR-23a	MAN2A2	1	1	1	1
104	hsa-miR-23a	MCM6	1	1	1	1
105	hsa-miR-23a	MEF2C	1	1	1	1
106	hsa-miR-23a	MEIS1	1	1	1	1
107	hsa-miR-23a	MYH4	1	1	1	1

108	hsa-miR-23a	PPP1R12A	1	1	1	1
109	hsa-miR-23a	NEB	1	1	1	1
110	hsa-miR-23a	NTS	1	1	1	1
111	hsa-miR-23a	NOX4	1	1	1	1
112	hsa-miR-23a	TMED7	1	1	1	1
113	hsa-miR-23a	KLF3	1	1	1	1
114	hsa-miR-23a	MEX3C	1	1	1	1
115	hsa-miR-23a	KLRF1	1	1	1	1
116	hsa-miR-23a	CDC40	1	1	1	1
117	hsa-miR-23a	CRLF3	1	1	1	1
118	hsa-miR-23a	PITPNA	1	1	1	1
119	hsa-miR-23a	PKNOX1	1	1	1	1
120	hsa-miR-23a	PLAU	1	1	1	1
121	hsa-miR-23a	AUH	1	1	1	1
122	hsa-miR-23a	C20orf11	1	1	1	1
123	hsa-miR-23a	CXorf57	1	1	1	1
124	hsa-miR-23a	MSL2L1	1	1	1	1
125	hsa-miR-23a	SLC25A36	1	1	1	1
126	hsa-miR-23a	AGPAT5	1	1	1	1
127	hsa-miR-23a	ZNF701	1	1	1	1
128	hsa-miR-23a	ZNF395	1	1	1	1

#, 1 represents the gene is predicted.

Supplementary Table 2. Sequence information for real time PCR primers used in described studies

Gene	Primers (5′→3′)	Product (bp)
RUNX2	F[1]: GCGCATTCCTCATCCCAGTA	176
	R[2]: GGCTCAGGTAGGAGGGGTAA	
CDH1	F: CAGGCTCAAGCTATCCTTGC	199
	R: GTGCAGTGGCTCATGTCTGT	
CDH2	F: TCAGTGGCGGAGATCCTACT	192
	R: CAGACACGGTTGCAGTTGAC	
TWIST1	F: GGACAGTGATTCCCAGACG	182
	R: GATGCCTTTCCTTTCAGTGG	
TIMP1	F: TGATGGTGGGTGGATGAGTA	203
	R: AACAACAGGATGCCAGAAGC	
SNAIL2	F: GAGCATTTGCAGACAGGTCA	205
	R: ATTTGGCTTCGGAGTGAAGA	
ZEB1	F: TCCAACCCGTGCTAACTACC	200
	R: TCCCTGCAATCAGAACTCAA	
ZEB2	F: CAGCTCTTCCACCTCAAAGC	194

	R: TCCTTGTTTCCGCTGGTACT	
ACTB	F: AGAAAATCTGGCACCACACC R: AGAGGCGTACAGGGATAGCA	188

Supplementary Table 3. Sequence information for siRNA used in described studies

ATG12	Sense: GUUGCAGCUUCCUACUUCATT Antisense: UGAAGUAGGAAGCUGCAACTT
ATG5	Sense: CCAUCAAUCGGAAACUCAUTT Antisense: AUGAGUUUCCGAUUGAUGGTT
RhoA	Sense: AUGGAAAGCAGGUAGAGUUTT Antisense: AACUCUACCUGCUUUCCAUTT
RUNX2	Sense-1: GGUCCUAUGACCAGUCUUATT Antisense-1: UAAGACUGGUCAUAGGACCTT Sense-2: CCAGCCACCUUUACUUACATT Antisense-2: UGUAAGUAAAGGUGGCUGGTT Sense-3: CACGCUAUUAAAUCCAAAUTT Antisense-3: AUUUGGAUUUAAUAGCGUGTT